CHIN. PHYS. LETT. Vol. 33, No. 8 (2016) 088102

Fabrication of GaN-Based Heterostructures with an InAlGaN/AlGaN Composite Barrier *

Ru-Dai Quan(全汝岱), Jin-Cheng Zhang(张进成)**, Jun-Shuai Xue(薛军帅), Yi Zhao(赵一), Jing Ning(宁静), Zhi-Yu Lin(林志宇), Ya-Chao Zhang(张雅超), Ze-Yang Ren(任泽阳), Yue Hao(郝跃)

Key Laboratory of Wide Band-Gap Semiconductor Technology, School of Microelectronics, Xidian University, Xi'an 710071

(Received 28 April 2016)

GaN-based heterostructures with an InAlGaN/AlGaN composite barrier on sapphire (0001) substrates are grown by a low-pressure metal organic chemical vapor deposition system. Compositions of the InAlGaN layer are determined by x-ray photoelectron spectroscopy, structure and crystal quality of the heterostructures are identified by high resolution x-ray diffraction, surface morphology of the samples are examined by an atomic force microscope, and Hall effect and capacitance–voltage measurements are performed at room temperature to evaluate the electrical properties of heterostructures. The Al/In ratio of the InAlGaN layer is 4.43, which indicates that the InAlGaN quaternary layer is nearly lattice-matched to the GaN channel. Capacitance–voltage results show that there is no parasitic channel formed between the InAlGaN layer and the AlGaN layer. Compared with the InAlGaN/GaN heterostructure, the electrical properties of the InAlGaN/AlGaN/GaN heterostructure are improved obviously. Influences of the thickness of the AlGaN layer on the electrical properties of the heterostructures are studied. With the optimal thickness of the AlGaN layer to be 5 nm, the 2DEG mobility, sheet density and the sheet resistance of the sample is 1889.61 $cm^2/V{\cdot}s$, 1.44×10^{13} cm^{-2} and as low as 201.1 Ω/sq, respectively.

PACS: 81.05.Bx, 81.05.Ea, 81.15.Gh, 81.15.Kk DOI: 10.1088/0256-307X/33/8/088102

Using InAlGaN quaternary barrier in GaN-based high-electron-mobility transistors (HEMTs) has attracted much attention nowadays.[1–4] By changing the composition, and hence the spontaneous and piezoelectric polarization in a pseudomorphically grown InAlGaN layer, polarization difference between the InAlGaN barrier and the GaN channel can be controlled,[5–8] and also with the Al/In ratio equal to 4.7, the InAlGaN barrier can be grown with lattice matching to the GaN channel, which is expected to reduce the density of strain-related defects and to improve the performance of HEMTs.[9–13] Nevertheless, the binary compositions (InN, GaN, AlN) of InAlGaN quaternary have large lattice mismatches with each other and correspondingly, have different favorite growth conditions, hence it is difficult to fabricate InAlGaN quaternary with high crystal quality.[14–16] Also, the alloy disorder scattering of InAlGaN quaternary is more severe than that of AlGaN ternary,[17] the expected high electron mobility cannot be achieved, which has limited the application of InAlGaN quaternary. For conventional AlGaN/GaN HEMTs, excellent electrical properties of high mobility and high sheet density of two-dimensional electron gas (2DEG) have been realized, but the stress and defects in the active layer due to the large lattice mismatch still affect the performance of the devices.[18–20] In this Letter, we propose GaN-based heterostructures with an InAlGaN/AlGaN composite barrier. The thin AlGaN layer grown on GaN template with high Al content provide excellent 2DEG and the InAlGaN quaternary grown subsequently on the AlGaN layer is lattice-matched to the GaN channel. This heterostructure is expected to combine the advantages of the InAlGaN and AlGaN barriers, meanwhile to neutralize the disadvantages.

The heterostructures were fabricated by the low-pressure metal-organic chemical vapor deposition (MOCVD) system on c-plane sapphire substrates. Triethylgallium (TEGa), trimethylaluminum (TMAl), trimethylindium (TMIn), and ammonia (NH_3) have been used as precursors of Ga, Al, In and N, respectively. First, a 1.4-μm-thick undoped GaN buffer layer was grown at 900℃ by the conventional two-step growth method on a sapphire (001) substrate, and a 1.2-nm-thick AlN interlayer was inserted to reduce the alloy disorder scattering and to improve the electron mobility. Subsequently, the lower AlGaN barrier with high Al content is deposited at the same temperature. Then, the reactor was cooled down to 700℃ for the deposition of upper InAlGaN quaternary barrier. The GaN, AlN and AlGaN layers were grown in ambient hydrogen, InAlGaN layers were grown in ambient nitrogen, and the reactor pressure was held at 40 torr during the whole growing process. The InAlGaN/AlGaN/GaN sample with the 5 nm AlGaN layer

*Supported by the National Science and Technology Major Project under Grant No 2013ZX02308-002, and the National Natural Science Foundation of China under Grant Nos 11435010, 61474086 and 61334002.

**Corresponding author. Email: jchzhang@xidian.edu.cn

© 2016 Chinese Physical Society and IOP Publishing Ltd

was fabricated and marked as A, an InAlGaN/GaN heterostructure was marked as B, and an AlGaN/GaN heterostructure was marked as C fabricated for comparison. The schematic diagrams are shown in Fig. 1.

After growth, the alloy compositions of the quaternary were determined by x-ray photoelectron spectroscopy (XPS), structure and crystal quality were assessed by high resolution x-ray diffraction (HRXRD), surface morphology was observed by an atomic force microscope (AFM) over a $5\times5\mu m^2$ scan area, and the electrical properties of the heterostructures were measured by capacitance–voltage (C–V) measurements and Hall effect measurements.

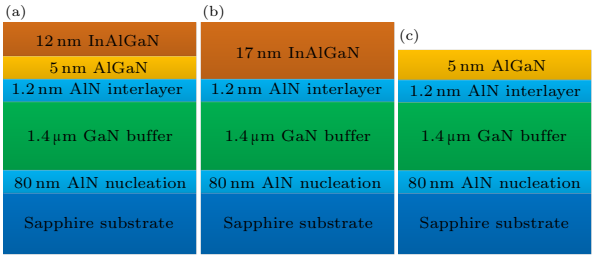

Fig. 1. Schematic diagrams view of (A) InAlGaN/AlGaN/GaN, (B) InAlGaN/GaN and (C) AlGaN/GaN heterostructures grown by MOCVD.

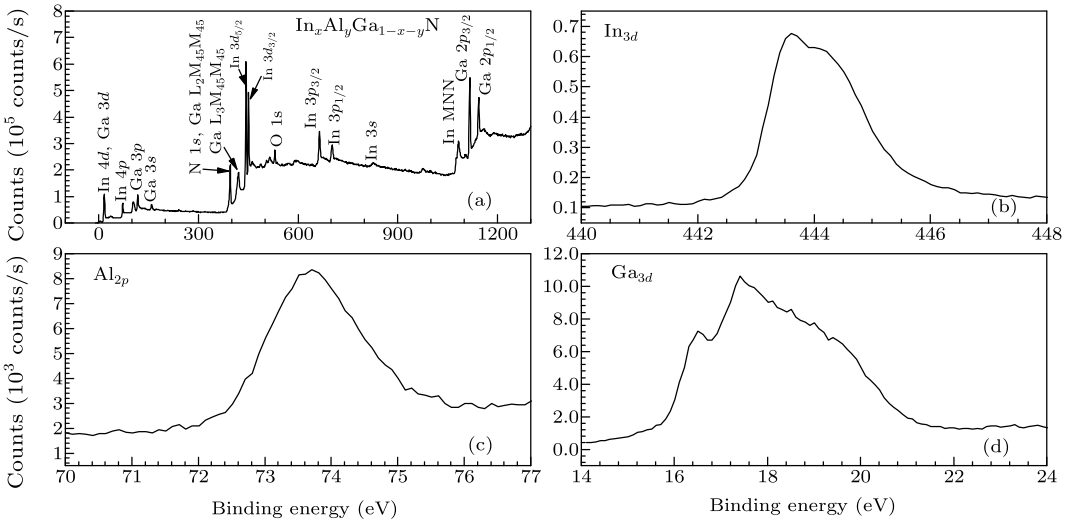

Fig. 2. (a) XPS survey spectrum of the InAlGaN quaternary layer. (b)–(d) High-resolution XPS spectra of the main signals related to the In, Al, Ga elements, respectively.

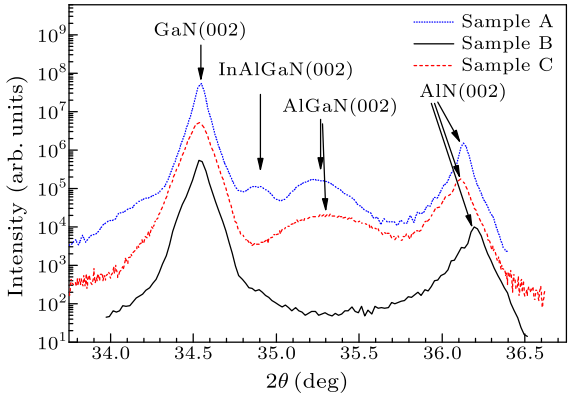

Fig. 3. HRXRD patterns of the InAlGaN/AlGaN/GaN, InAlGaN/GaN and AlGaN/GaN heterostructures.

To determine the composition content of the InAlGaN quaternary, XPS measurements were realized. Figure 2(a) shows a survey XPS spectrum of the InAlGaN quaternary. Before the scan, the sample was etched by Ar^+ for 30 s at 1200 eV to get rid of O and C elements absorbed on the surface which was produced in the sample transfer process. From this spectrum, we can find fifteen photoelectron signals corresponding to the elements In, Al, Ga, N and O. This can also prove that the InAlGaN quaternary was deposited successfully. As the sample has been etched, the existence of O_{1s} signal is mainly due to the decomposition of the Al_2O_3 substrate in high temperature and residual oxygen in carrier gas. The compositions of the InAlGaN quaternary alloy were obtained by quantitative analyses calculated by the test software from high-resolution XPS spectra of In_{3d}, Al_{2p}, Ga_{3d} signals and compositions are 14.62%, 64.78% and 20.60% for InN, AlN and GaN, respectively. The ratio of AlN to InN is 4.43, which indicates that the InAlGaN layer is nearly lattice matched to the GaN channel.

The HRXRD results of samples A, B and C are shown in Fig. 3. The dominating peak at an angle of 34.5° corresponds to the underlying GaN channel and the peak at the angle of 36.2° corresponds to the AlN nucleating layer. The peaks located between 34.5° and 36.2° correspond to the barrier layer. The shape of peaks of GaN and AlN indicates the high crystal quality of the GaN buffer and the AlN nucleating layer. Comparing sample A with sample C, we can confirm that the broad diffraction peaks at an angle of 35.4° correspond to the AlGaN layer. Therefore, the diffraction peaks at an angle of 34.9° in the diffraction spectrum of sample A correspond to

the InAlGaN quaternary. There is no obvious InAlGaN quaternary diffraction peak in sample B. This may be due to the inferior crystal quality as the InAlGaN quaternary was directly grown on GaN buffer. From the diffraction spectrum, the Al content in the AlGaN layer was estimated as high as 46%–51%, using Bragg's law, Vegard's law and $c_{\mathrm{AlN}} = 0.498\,\mathrm{nm}$, $c_{\mathrm{GaN}} = 0.518\,\mathrm{nm}$.[21,22] The AlN diffraction peaks in samples A and C shift to lower 2θ degree. It is caused by the variation of tensile stress between the AlN nucleating layer and GaN buffer which is induced by the fluctuation of growth conditions.

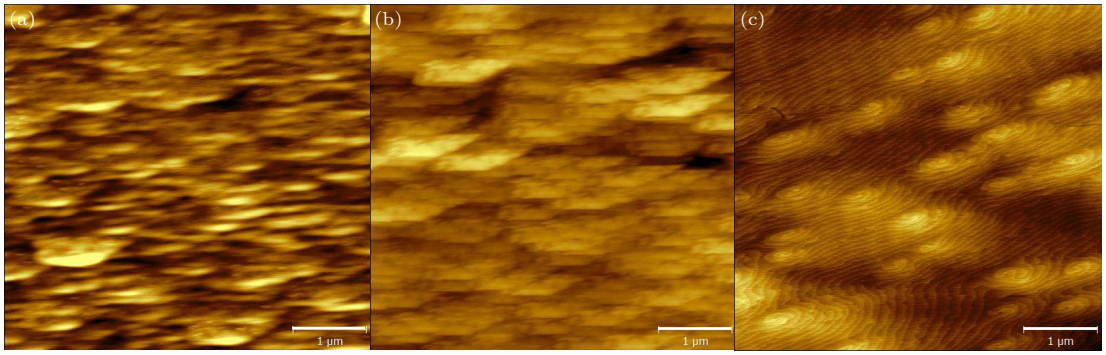

Fig. 4. AFM images of the three heterostructure samples (a) InAlGaN/GaN/GaN, rms roughness 3.43 nm, (b) InAlGaN/GaN, rms roughness 4.67 nm, and (c) AlGaN/GaN, rms roughness 0.41 nm.

Surface morphologies of samples A, B and C were examined by the AFM. The $5 \times 5\,\mu\mathrm{m}^2$ images are displayed in Fig. 4. For the two samples with InAlGaN quaternary, no obvious multilayer steps are found. This indicates that the growth model of the two samples is an island growth model rather than a step-flow model. Compared with sample B (rms roughness 4.67 nm), the rms roughness of sample A is 3.43 nm, which means that the insertion of the AlGaN layer can improve the surface morphology of the samples, while it is still relatively larger than the conventional AlGaN/GaN heterostructure (0.41 nm). It is mainly due to the relatively low growth temperature for the InAlGaN quaternary layer which results in low mobility of the absorbed atom. For sample C, the surface morphology suggests the typical spiral growth mode, in which the growth terraces and the outcrops of a screw are clearly observed, similar to the report of Shang *et al.*[23] The appearance of the heliciform island is ascribed to the low Al atom surface mobility and relatively high Al content.

It is very important to understand the carrier distribution in the InAlGaN/AlGaN/GaN heterostructure, therefore C–V measurements were carried out and the results are plotted in Fig. 5. It is observed that with the increase of the bias voltage, the capacitance plateaus appear at the pinch-off voltages of −5.4 V, corresponding to the decrease amount and complete depletion of the confined 2DEG density. The 2DEG peaks are sharp, with carrier concentrations of $9.2 \times 10^{19}\,\mathrm{cm}^{-3}$ located at 18 nm below the surface of the sample. This conduction channel is corresponding to the 2DEG channels at the AlGaN-GaN interface. Furthermore, no parasitic conduction channel is observed at the InAlGaN-AlGaN interface. This may be due to the small conduction band discontinuity between the two layers.

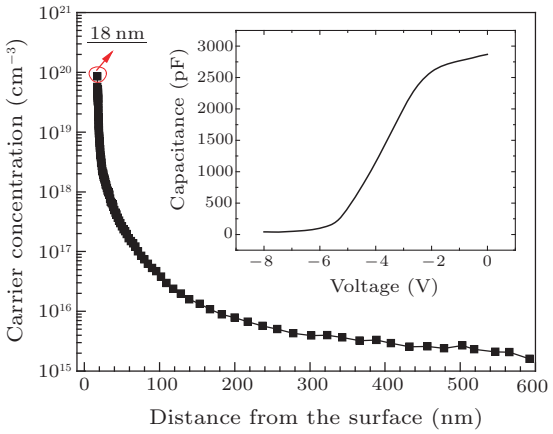

Fig. 5. The C–V characteristics of the InAlGaN/AlGaN/GaN heterostructure.

Hall effect measurements were performed at room temperature to investigate the electrical properties of the heterostructures. As presented in Table 1, compared with sample B, the electrical properties of the InAlGaN/AlGaN/GaN heterostructure are greatly improved. The high mobility of 2DEG is ascribed to the smooth AlGaN-GaN interface and the high 2DEG sheet density is caused by the strong spontaneous polarization field which is induced by the high Al content in the AlGaN layer.

The influences of AlGaN layer's thickness on electrical properties of the heterostructures have also been studied, the results are listed in Table 2. As the thickness of the AlGaN layer increases from 2 nm to 5 nm, the mobility of 2DEG increases from $1397.7\,\mathrm{cm}^2/\mathrm{V{\cdot}s}$ to $1889.6\,\mathrm{cm}^2/\mathrm{V{\cdot}s}$. This is mainly due to the reduction of InAlGaN quaternary disorder scattering effect as the distance between the InAlGaN layer and the GaN channel increases. As the AlGaN layer increases

from 5 nm to 7 nm, the mobility of 2DEG decreases to 1795.4 $cm^2/V{\cdot}s$. This is mainly due to the crystal quality deterioration of the AlGaN layer, which is caused by the strain relaxation and formation of dislocations as the thickness of AlGaN layer exceeds the critical value.[24] With the optimal thickness of 5 nm of the AlGaN layer, the heterostructure has the lowest sheet resistance of 201.1 Ω/sq.

Table 1. Electrical properties of three kinds of heterostructures.

Sample ID	Mobility ($cm^2/V{\cdot}s$)	Sheet density ($10^{13}\,cm^{-2}$)	Resistance (Ω/sq)
A	1889.6	1.44	201.1
B	753.1	1.33	622.2
C	1503.4	1.85	224.6

Table 2. Electrical properties of InAlGaGaN/AlGaN/GaN heterostructures with different AlGaN layer thicknesses.

AlGaN layer thickness (nm)	Mobility ($cm^2/V{\cdot}s$)	Sheet density ($10^{13}\,cm^{-2}$)	Resistance (Ω/sq)
2	1397.7	1.74	257.1
5	1889.6	1.44	201.1
7	1795.4	1.67	225.3

In summary, we have proposed a new structure using an InAlGaN/AlGaN composite layer as the barrier layer, and the influences of the thickness of the AlGaN layer on the electrical properties of the heterostructures are studied. As the InAlGaN quaternary layer is nearly lattice-matched to the GaN channel, the C–V results show that there is no parasitic channel formed between the InAlGaN layer and the AlGaN layer. Compared with the InAlGaN/GaN heterostructure, the electrical properties of the InAlGaN/AlGaN/GaN heterostructure are improved obviously. With the optimal thickness of 5 nm of the AlGaN layer, the 2DEG mobility of the sample is 1889.61 $cm^2/V{\cdot}s$, the sheet density is $1.44\times10^{13}\,cm^{-2}$ and the sheet resistance is as low as 201.1 Ω/sq.

References

[1] Lim T, Aidam R, Waltereit P, Henkel T, Quay R, Lozar R, Maier T, Kirste L and Ambacher O 2010 *IEEE Electron Device Lett.* **31** 671

[2] Wang R H, Li G W, Verma J, Berardi S R, Fang T, Guo J, Hu Z Y, Laboutin O, Cao Y, Johnson W, Snider G, Fay P, Jena D and Xing H L 2011 *IEEE Electron Device Lett.* **32** 1215

[3] Lu H M, Chen G X and Jian S S 2009 *Chin. Phys. Lett.* **26** 087803

[4] Husnain G, Chen T X, Tao F and Yao S D 2010 *Chin. Phys. B* **19** 087205

[5] Quan R D, Zhang J C, Xu S R, Xue J S, Zhao Y, Ning J, Lin Z Y, Ren Z Y and Hao Y 2016 *Chin. Phys. Lett.* **33** 048101

[6] Ambacher O, Majewski J, Miskys C, Link A, Hermann M, Eickhoff M, Stutzmann M, Bernardini F, Fiorentini V, Tilak V, Schaff B and Eastman L F 2002 *J. Phys.: Condens. Matter* **14** 3399

[7] Choi S, Kim H J, Lochner Z, Zhang Y, Lee Y C, Shen S C, Ryou J H and Dupuis R D 2010 *Appl. Phys. Lett.* **96** 243506

[8] Reuters B, Wille A, Ketteniss N, Hahn H, Hollander B, Heuken M, Kalisch H and Vescan A 2013 *J. Electron. Mater.* **42** 826

[9] Nakazawa S, Ueda T, Inoue K, Tanaka T, Ishikawa H and Egawa T 2005 *IEEE Trans. Electron Devices* **52** 2124

[10] Lim T, Aidam R, Kirste L, Waltereit P, Quay R, Müller S and Ambacher O 2010 *Appl. Phys. Lett.* **96** 252108

[11] Xue J S, Hao Y, Zhang J C,. Zhou X W, Liu Z Y, Ma J C and Lin Z Y 2011 *Appl. Phys. Lett.* **98** 113504

[12] Xue J S, Zhang J C, Hou Y W, Zhou H, Zhang J F and Hao Y 2012 *Appl. Phys. Lett.* **100** 013507

[13] Choi S, Wu F, Shivaraman R, Young E C and Speck J S 2012 *Appl. Phys. Lett.* **100** 232102

[14] Takayama T, Yuri M, Itoh K, Baba T and Harris J S 2001 *J. Cryst. Growth* **222** 29

[15] Yasan A, McClintock R, Mayes K, Darvish S R, Zhang H, Kung P, Razeghi M, Lee S K and Han J Y 2002 *Appl. Phys. Lett.* **81** 2151

[16] Shang J Z, Zhang B P, Mao M H, Cai L E, Zhang J Y, Fang Z L, Liu B L, Yu J Z, Wang Q M, Kusakabe K and Ohkawa K 2009 *J. Cryst. Growth* **311** 474

[17] Li Y, Zhang J F, Wan W, Zhang Y C, Nie Y H, Zhang J C and Hao Y 2015 *Physica* E **67** 77

[18] Liu Y, Egawa T, Ishikawa H and Jimbo T 2003 *J. Cryst. Growth* **259** 245

[19] Wu J J, Li D B, Lu Y, Han X X, Li J M, Wei H Y, Kang T T, Wang X H, Liu X L, Zhu Q S and Wang Z G 2004 *J. Cryst. Growth* **273** 79

[20] Goto O, Tomiya S, Hohshina Y, Tanaka T, Ohta M, Ohizumi Y et al 2007 *Proc. SPIE* **6485** 64850Z

[21] Tanaka M, Nakahata S, Sogabe K, Nakata H and Tabioka M 1997 *Jpn. J. Appl. Phys.* **36** L1062

[22] Paszkowicz W 1999 *Powder Diffr.* **14** 258

[23] Shang J Z, Zhang B P, Wu C M, Cai L E, Zhang J Y, Yu J Z and Wang M 2008 *Appl. Surf. Sci.* **255** 3350

[24] Fischer A, Kiihne H and Richter H 1994 *Phys. Rev. Lett.* **73** 2712